ELSEVIER

2 September 2002

Physics Letters A 301 (2002) 413–423

PHYSICS LETTERS A

www.elsevier.com/locate/pla

Detection of nonlinearity and chaoticity in time series using the transportation distance function

Sukanta Basu *, Efi Foufoula-Georgiou

University of Minnesota, St. Anthony Falls Laboratory, Mississippi River at 3rd Ave. SE, Minneapolis, MN 55414, USA

Received 27 November 2001; received in revised form 7 May 2002; accepted 25 July 2002

Communicated by A.P. Fordy

Abstract

We propose a systematic two-step framework to assess the presence of nonlinearity and chaoticity in time series. Although the basic components of this framework are from the well-known paradigm of surrogate data and the concept of short-term predictability, the newly proposed discriminating statistic, the *transportation distance function* offers several advantages (e.g., robustness against noise and outliers, fewer data requirements) over traditional measures of nonlinearity. The power of this framework is tested on several numerically generated series and the Santa Fe Institute competition series.

PACS: 05.45.a; 05.45; 05.45.t

Keywords: Chaos; Nonlinearity; Short-term prediction; Surrogate data; Time series; Transportation distance

1. Introduction

Given an observed time series, the usual procedure to discriminate whether this series comes from a deterministic chaotic system versus a random (stochastic) process is to estimate the attractor dimension following the Grassberger–Procaccia (GP) correlation dimension algorithm [8] and to infer the underlying process based on that dimension. However, there are several problems associated with this algorithm, for example, large data requirements, stationarity, presence of noise, lacunarity and edge effects [2]. Moreover, given a strange attractor, a finite correlation dimension follows, but there exists no converse theorem [18,26]. Like dimensions, a number of other measures (e.g., entropies, Lyapunov exponents) have been developed based on concepts from nonlinear dynamics and theory of deterministic chaos, which possess similar problems [16].

Instead of relying on the dimension estimates of the underlying attractor, several authors advocated the concept of short-term predictability to distinguish randomness from chaos [12,22]. The basic idea is that, chaotic systems follow definite rules, and accurate short-term predictions are possible although the predictability decreases exponentially with time due to the extreme sensitivity on initial conditions [3]. Sugihara and May [22] proposed a short-term prediction method based on a library of patterns in time series. A flat distribution of the correlation coefficient be-

* Corresponding author.
E-mail address: basu0009@tc.umn.edu (S. Basu).

0375-9601/02/$ – see front matter
PII: S0375-9601(02)01083-6

tween the predicted and original series versus prediction horizon indicates uncorrelated noise, whereas in the case of chaos such a plot would display a gradual fall off [2,22]. However, this method may fail on correlated noise, as even in this case, the correlation coefficient can be higher for short times than for long [12]. Kennel and Isabelle [12] also used short-term predictability as a tool to discriminate deterministic chaos from randomness. They compared the prediction error of a given time series to the prediction errors of an ensemble of random time series which have the same average power spectral density as the original data series. Casdagli [4] suggested the Deterministic versus Stochastic (DVS) algorithm based on local linear models [5]. He computed average forecast error as a function of the neighborhood size. A small value of neighbors corresponds to a deterministic nonlinear system, whereas, a larger value of neighbors corresponds to a stochastic process or a deterministic process with high dimension [4,5].

Since nonlinearity is a necessary condition for chaoticity [6], several researchers attempted mere detection of nonlinearity, instead of positive identification of chaotic dynamics. As mentioned by Paluš [16], the detection of nonlinearity itself is not a trivial task and there are various sources of possible errors in nonlinearity testing. One of the most popular nonlinearity detection methods is based on "surrogate data" [23]. This method provides a rigorous statistical test for the null hypothesis that the data have been generated by a linear stochastic process [19]. Deviations from the null hypothesis can be detected by comparing some measure of nonlinearity computed from the data with that computed from a number of Monte Carlo realizations of a linear stochastic process (the surrogates). The original time series and the surrogates must have the same autocorrelation function or, equivalently, the same power spectrum. In the case of nonlinearity testing of linear stochastic dynamics distorted by simple nonlinear rescaling (static nonlinearity), the single time probability distribution also must be conserved [11,19]. Schreiber and Schmitz [20] compared the performance of a number of different measures of nonlinearity (a maximum likelihood estimator of the GP correlation dimension, modified Brock–Dechert–Scheinkman statistic, nonlinear prediction error with respect to a locally constant predictor, higher-order autocovariance and time reversibility). They found that the root-mean-squared error of the locally constant predictor gave consistent good discriminatory power. Other nonlinearity measures gave better performances in some cases, but failed in others.

Diks et al. [6] used "reversibility" as a criterion to discriminate between time series. A time series is said to be reversible if its probabilistic properties are invariant with respect to time reversal. If the null hypothesis of reversibility can be rejected, a linear Gaussian random process can be excluded as the generating mechanism [6]. However, as Schreiber and Schmitz [20] mentioned, asymmetry under time reversal is a sufficient and powerful indicator of nonlinearity, but not a necessary condition.

Paluš [15,16] presented a method for testing nonlinearity based on information-theoretic functional redundancies. In a later work, Paluš [17] introduced the concept of coarse-grained entropy rates (CERs), also computed from information-theoretic functionals-redundancies. The CERs are relative measures of regularity and predictability, and for data generated by dynamical systems they are related to Kolmogorov–Sinai entropy. If one dataset gives higher CER than the other, the former is more irregular and less predictable than the latter [17].

Recently, Bhattacharya and Kanjilal [2] proposed a new determinism detection method based on the Singular Value Decomposition. Chaoticity manifests in the relatively decreasing strengths of the weaker modes with increasing dimension of the orthogonal spaces mapping the process. They used surrogates to discriminate between chaoticity and stochasticity. However, Bhattacharya and Kanjilal [2] commented, "In spite of these available approaches, a clear differentiation between chaotic and stochastic process seems to be rather problematic".

In this Letter, we propose a two-step framework to detect first nonlinearity and then chaoticity based on the ideas of transportation distance function [14], surrogate data and short-term predictability. The transportation distance function, the workhorse of our framework, is based on both the geometric and probabilistic aspects of point distributions and can provide a measure of long term qualitative differences between any two time series. From this point of view, it is superior to simple correlation coefficient or root-mean-squared error. Apart from the inherent abilities of the

transportation distance function, the framework has several other merits that will be discussed in Section 3.

To enhance the readability of the Letter, we have briefly summarized the ideas of the transportation distance in Section 2. Section 3 delineates the nonlinearity and chaoticity detection framework. To demonstrate its potential we have applied this framework to a wide variety of time series and Section 4 describes the results for several numerically generated time series. In Section 5 the method is applied to the Santa Fe Institute competition series [7].

2. Transportation distance function

Moeckel and Murray [14] used the transportation distance function $d(x, y)$ to measure the "distance" between time series (x and y), where distance reflects the difference in the long-term behavior. The idea was to develop a distance function, that would give small values when the systems generating x and y have similar attractors or nearby probability distributions in the phase space.

In practice, the scalar time series x and y are transformed into vector time series X and Y respectively by phase space reconstruction with an integer delay (τ) and embedding dimension (e). This results in an e-dimensional embedding space $\mathbb{R}^e$ in which the dynamics of the x and y systems' attractors are captured. Then, a box in $\mathbb{R}^e$ containing both embedded time series (X and Y) is divided into finitely many sub-boxes $B_i, i = 1, \ldots, b$. Let, $p_i = P(B_i)$ and $q_i = Q(B_i)$. The probability vectors $p = (p_1, \ldots, p_b)$ and $q = (q_1, \ldots, q_b)$ represent the discretized probability measures. A transportation plan would specify the amount of material to ship between each pair of boxes. Let, $\mu_{ij} \geqslant 0$ be the amount shipped from box B_i to box B_j according to a transportation plan, μ. To preserve the initial and final distributions, we require that:

$$\sum_{j=1}^{b} \mu_{ij} = p_i, \quad i = 1, \ldots, b, \tag{1}$$

$$\sum_{i=1}^{b} \mu_{ij} = q_j, \quad j = 1, \ldots, b. \tag{2}$$

Let $M(p, q)$ be the set of all transportation plans satisfying these constraints. Then the transportation distance is obtained by minimizing the transportation cost:

$$d(p, q) = \inf_{\mu \in M(p,q)} \sum_{i,j=1}^{b} \mu_{ij} \delta_{ij}, \tag{3}$$

where δ_{ij} is the taxi cab metric normalized to the embedding dimension between the centres of B_i and B_j.

Moeckel and Murray [14] replaced this transportation problem by an equivalent transshipment problem and computed the transportation distance (d) efficiently by the network simplex algorithm.

This distance function has several advantages. It is based on both geometrical and probabilistic factors (thus superior to the total variation distance) and less sensitive to outliers, noise and discretization errors (thus better than the Hausdorff distance). Moreover, it can be used in any embedding dimension and systems with similar attractors should produce small values of d in every dimension. However, it is possible for systems to appear similar in one dimension and dissimilar in a higher dimension.

3. Nonlinearity and chaoticity detection framework

The proposed framework consists of two logical steps. The first step is to detect nonlinearity based on the method of surrogate data using the transportation distance function. The surrogates are generated following any available methodology, e.g., by implementing the iterative Fourier based scheme introduced by Schreiber and Schmitz [19]. The transportation distances are first computed between the original data set $\{x_n^o\}$ and all the surrogate data sets $\{x_n^i\}, i = 1, \ldots, N_s$:

$$d_{oi}\left(x_n^o, x_n^i\right), \quad i = 1, \ldots, N_s. \tag{4}$$

In a similar way, the mutual distances between the surrogates are computed:

$$d_{ij}\left(x_n^i, x_n^j\right), \quad i, j = 1, \ldots, N_s \quad \text{and} \quad i \neq j. \tag{5}$$

It is ideal to perform all the transportation distance computations for the optimal embedding dimension (the dimension computed by the false nearest neighbors algorithm [1,11]). When this is not computationally feasible, smaller embedding dimensions have to

be used as a compromise. Throughout this Letter embedding dimensions $e = 1, 2$ and 3 have been used. But, since in the case of surrogate generation the single time probability distribution is conserved, $e = 1$ in step one will always yield zero distance, as expected. We propose that, if for all the embeddings, the two distributions (d_{oi} and d_{ij}) are roughly non-overlapping, the null hypothesis of linear stochasticity can be rejected, and the original data can be considered to be nonlinear at this significance level.

The second step is to detect chaoticity based on the concept of short-term predictability. Given the original scalar data, a suitable delay time and an embedding dimension are chosen following the ideas of mutual information [1,11] and false nearest neighbors [1,11], respectively. In this delay embedding space, k-step ahead prediction is simply the average over the futures of the neighbors [11]:

$$\hat{x}_{n+k} = \frac{1}{N_{u_n}} \sum_{x_j \in u_n} x_{j+k}, \tag{6}$$

where N_{u_n} denotes the number of elements in the neighborhood u_n.

We apply this simple locally constant (zeroth order) predictor on every vector of the original series $\{x_n^o\}$ to obtain a k-step ahead predicted series $\{x_n^k\}$ (no iterated predictions). The transportation distances are calculated between the original series and k-step ahead predicted series for different embeddings as follows:

$$d_{ok}\left(x_n^o, x_n^k\right), \quad k = 1, \ldots, K, \tag{7}$$

We would like to emphasize that, the lags and embedding dimensions used in this framework for the short-term prediction should not be confused with the lags (always equal to 1) and embedding dimensions (always $e = 1, 2$ and 3) used for the transportation distance computations. The quality of short-term predictions highly depends on the proper selection of lag and embedding dimension, but as mentioned in Section 2, the characteristic behavior of the transportation distance is independent of embedding dimensions.

We conjecture that for all embedding dimensions the distance between the original and predicted series increases with prediction horizon in the case of deterministic chaos, whereas in the case of nonlinear stochastic processes there exists no such monotonic increasing behavior. It is appropriate at this point to elaborate on some subtleties arising in the definition of nonlinear stochastic processes and specifically on the transition spectrum between deterministic and nonlinear stochastic systems. Theoretically, any deterministic (chaotic or non-chaotic) system with a small amount of dynamical noise is infinite-dimensional (nonlinear stochastic). However, in practical sense if the noise is weak, its influence on the deterministic dynamics will be weak too so that the system will be close to the deterministic end of the spectrum. Such a system is frequently referred to in the literature as "approximately deterministic" [5]. It will be shown later (see Example 8 in Section 5) that such a system (deterministic chaotic with small amount of dynamical noise) will be correctly identified as chaotic by our framework. On the other hand, when noise is more dominant than its deterministic counterpart, the system can be termed as "nonlinear stochastic" and this is the definition used in this Letter. For such systems, our framework is shown (see Example 5 in Section 4) to correctly infer the absence of deterministic dynamics.

It is noted that, the monotonic profile of the transportation distance with lead-time is not a unique discriminant of chaotic processes and that long memory nonlinear stochastic processes can show a similar behavior. Also, in the case of certain noisy limit cycles it is possible to get a monotonically increasing profile up to the dominant oscillation zone (see Example 6 in Section 4) with a non-monotonic profile afterwards. On the other hand, some chaotic processes may not show any monotonic profile at all. For example, recently Bhattacharya and Kanjilal [3] showed that correlation coefficient versus prediction horizon profile might result in incorrect inferences for cyclical chaotic processes because of its non-monotonic behavior. One of the advantages of the proposed two-stage framework is that, the first step can eliminate the linear correlated processes which otherwise can "fool" the short-term predictability tests because of their long memories. Moreover, from our perspective, comparing two distributions (between the original series and the surrogate series (OS) and the mutual distances between the surrogates (MS)) is more rigorous than comparing one single value (statistic computed from the original time series) with a whole distribution (probability distribution calculated from surrogates).

Although, the second step of the proposed framework is very similar to that of Sugihara and May [23]

and is widely used in the literature, we acknowledge that it is not as robust (or foolproof) as the first step of our framework. This step allows one to separate nonlinear stochastic processes from nonlinear deterministic-chaotic processes, which is generally difficult in frameworks based only on the method of surrogate data. Conceptually, one can only use the first step of our framework to directly discriminate between non-chaotic processes and chaotic processes with the help of "tailor-made" surrogates (properly termed as constrained randomized surrogates [21]) constructed to test the presence of specific non-chaotic stochastic structures in a process.

Last but not least, the use of the transportation distance function is very general because it is defined not only for deterministic processes but for stochastic processes as well. In the next section, the robustness and potential of the proposed method is demonstrated on numerically generated series of known structure.

4. Numerically generated time series

All the numerically generated series are 10 000 points long, starting after 1000 points to avoid transient behavior. The number of boxes used for discretization of the phase space was $b = 100$ for embedding dimension $e = 1$, $b = 50^2 = 2500$ for $e = 2$ and $b = 20^3 = 8000$ for $e = 3$. The tests were carried out with nine surrogate series (90% level of significance for one-sided test) to reduce the computational burden. The implementation of the following algorithms: the mutual information, the false nearest neighbors approach, surrogate data generations and k-step predictions were done using the TISEAN package [9]. Table 1 gives a summary of all the parameters (for k-step predictions) of the time series.

Table 1
Characteristics of the generated time series

Example	Length	Lag	Embedding dimension	Neighborhood size (fraction of the standard deviation)
1	10 000	–	–	–
2	10 000	10	3	0.3
3	10 000	14	8	0.4
4	10 000	10	9	0.3
5	10 000	3	7	0.3
6	10 000	40	3	0.3
7	9 000	2	4	0.3
8	10 000	8	6	0.3

Example 1. Autoregressive model

First we consider a simple linear stochastic process (Fig. 1(a)):

$$x_n = 0.99x_{n-1} + \eta_n, \tag{8}$$

where η_n is independent Gaussian random noise with zero mean and unit variance. Fig. 1(a) depicts a realization of the time series. Fig. 1(b) and (c) show the two transportation distance distributions (OS and MS) for $e = 2$ and $e = 3$, respectively. Evidently, the distributions are highly overlapping, leading to the right conclusion of the non-rejection of the null hypothesis of linear stochasticity.

Example 2. Lorenz series

The Lorenz series for x (velocity of the fluid) results from the numerical solution of the Lorenz system of equations:

$$\frac{dx}{dt} = \sigma(y - x), \qquad \frac{dy}{dt} = -xz + rx - y,$$
$$\frac{dz}{dt} = xy - bz. \tag{9}$$

Here an explicit Runge–Kutta $(4, 5)$ formula, the Dormand–Prince pair [13] was used to solve the above equations (at each 0.01 time interval) for $\sigma = 16$, $b = 4$ and $r = 45.92$ [1]. Fig. 2(b) (top row) depicts the transportation distance distributions OS and MS. Clear separation of the distributions implies the presence of strong nonlinearity in the Lorenz series. After detecting the nonlinearity, the second step of the framework is applied: the short-term predictability test. The parameters $\tau = 10$ and $e = 3$ are chosen for the locally constant prediction. Fig. 2(c) (top row) shows the transportation distance versus prediction horizon profile. The monotonic increase of the distance between the original data series and the k-step predicted series attests to the chaoticity known to exist in the Lorenz series.

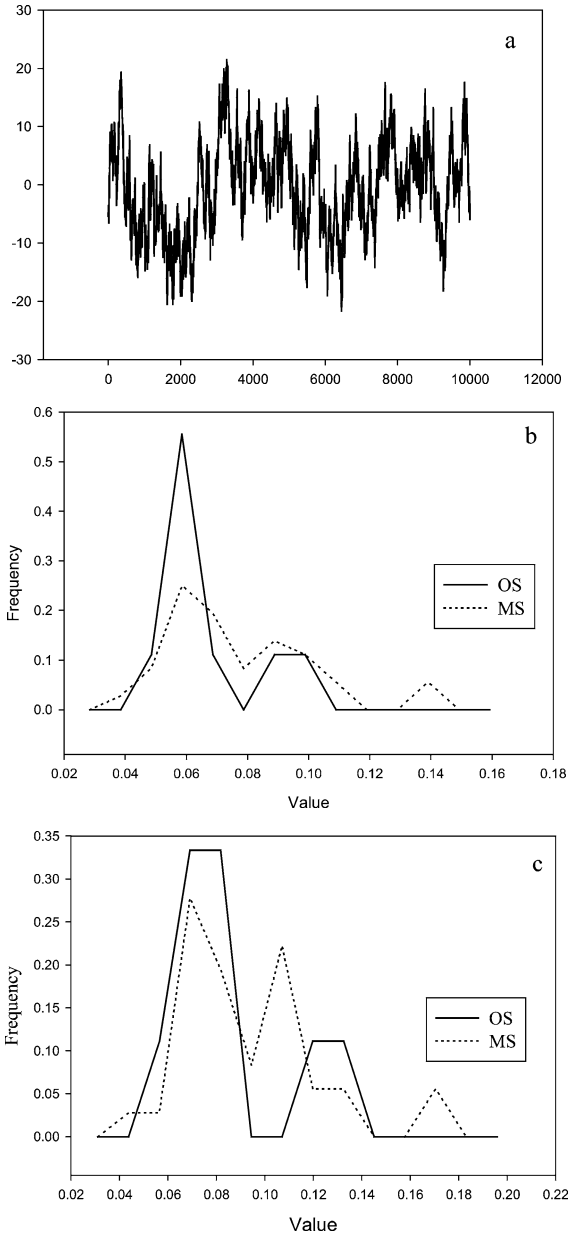

Fig. 1. Autoregressive process: (a) time series, (b) transportation distance function distributions ($e = 2$) and (c) transportation distance function distributions ($e = 3$).

Example 3. Noisy Lorenz series

Next we consider the same Lorenz series but with 30% (of standard deviation) additive Gaussian noise (Fig. 2(a), bottom row). Results of the step one procedure are shown in Fig. 2(b) (bottom row). Approximate separation of the distributions shows the robustness of this nonlinearity detection method against noise. Finally, Fig. 2(c) (bottom row) clearly captures the underlying chaoticity of the noisy Lorenz series.

Example 4. Nonlinearly distorted autoregressive process

In this example we consider the same linear stochastic AR-1 series (Example 1) but we distort the original series by a nonlinear measurement function (static nonlinearity):

$$y_n = x_n^3, \qquad x_n = 0.99x_{n-1} + \eta_n. \tag{10}$$

The series (Fig. 3(a)) looks very "spiky" and quite complicated [11,21]. Step one of our framework detects nonlinearity (Fig. 3(b)). Step two leads correctly to the rejection of any claim of chaoticity in the dynamics (Fig. 3(c) does not show any monotonic increasing behavior). In this case, the selection of lag time was arbitrary since the result from the mutual information algorithm was not conclusive. It is seen that the proposed framework fails to differentiate between distorted (by static nonlinearity) linear stochastic processes and nonlinear stochastic processes, because it is actually designed to detect chaoticity in the data, which it does correctly.

Example 5. Noisy sine limit cycle

The time series (Fig. 4(a)) is generated by adding 50% uniform noise from the interval $[-0.5, 0.5]$ independently at each step to a sine wave of unit amplitude ($x_t = \sin(0.5t)$) [22]. Fig. 4(b) depicts inherent nonlinearity and Fig. 4(c) strongly suggests nonchaotic behavior of the series. This is an example of a noisy limit cycle in which noise dominates and masks any characteristic signature of the deterministic component.

Example 6. Stochastic Van der Pol oscillator

This example deals with the Van der Pol oscillator (Fig. 5(a)):

$$\frac{dx_1}{dt} = x_2, \qquad \frac{dx_2}{dt} = \mu\left(1 - x_1^2\right) - x_1 + \varepsilon, \tag{11}$$

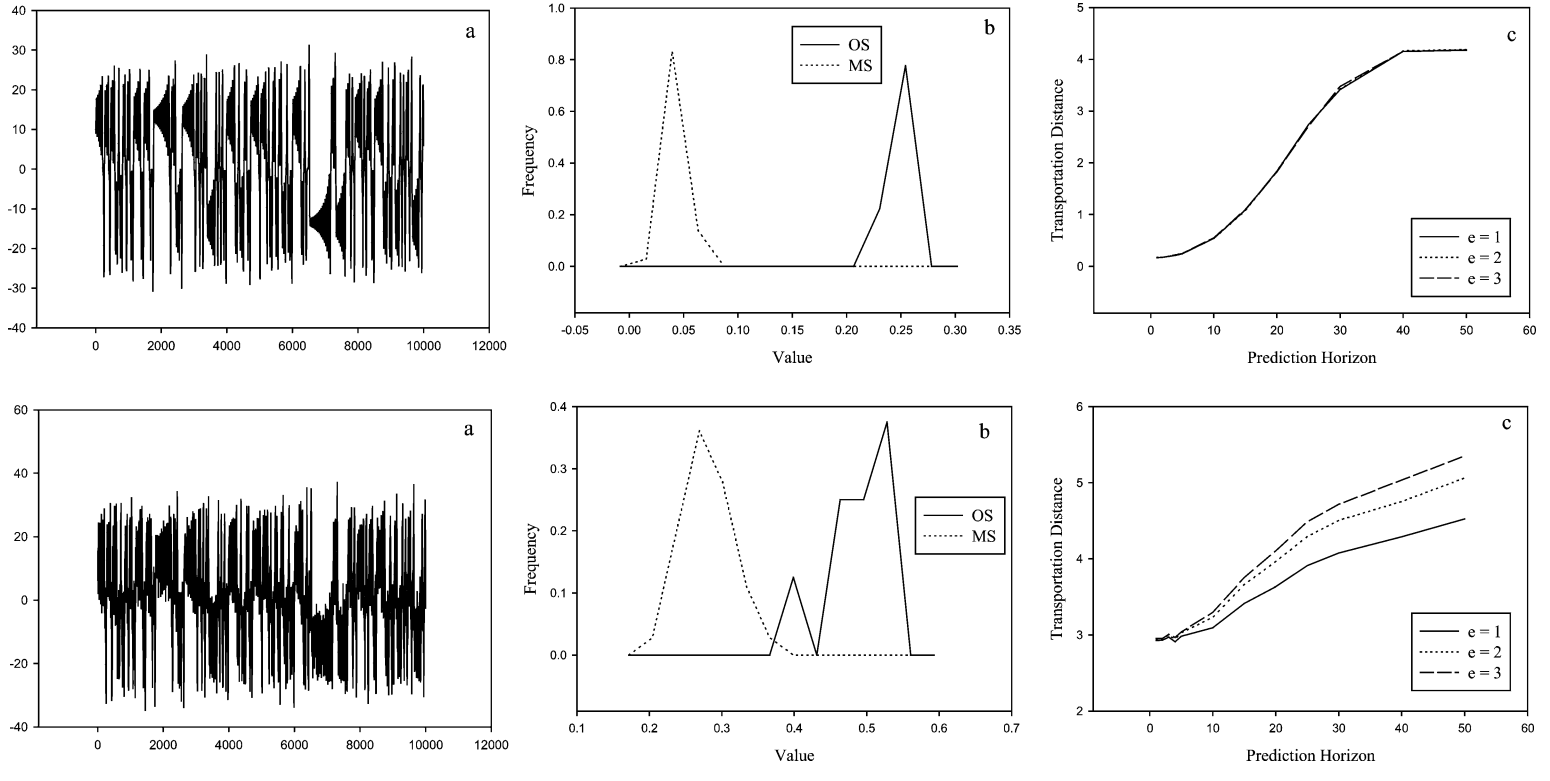

Fig. 2. Lorenz series (top row) and noisy Lorenz series (bottom row): (a) time series, (b) transportation distance function distributions ($e = 3$) and (c) k-step prediction profile.

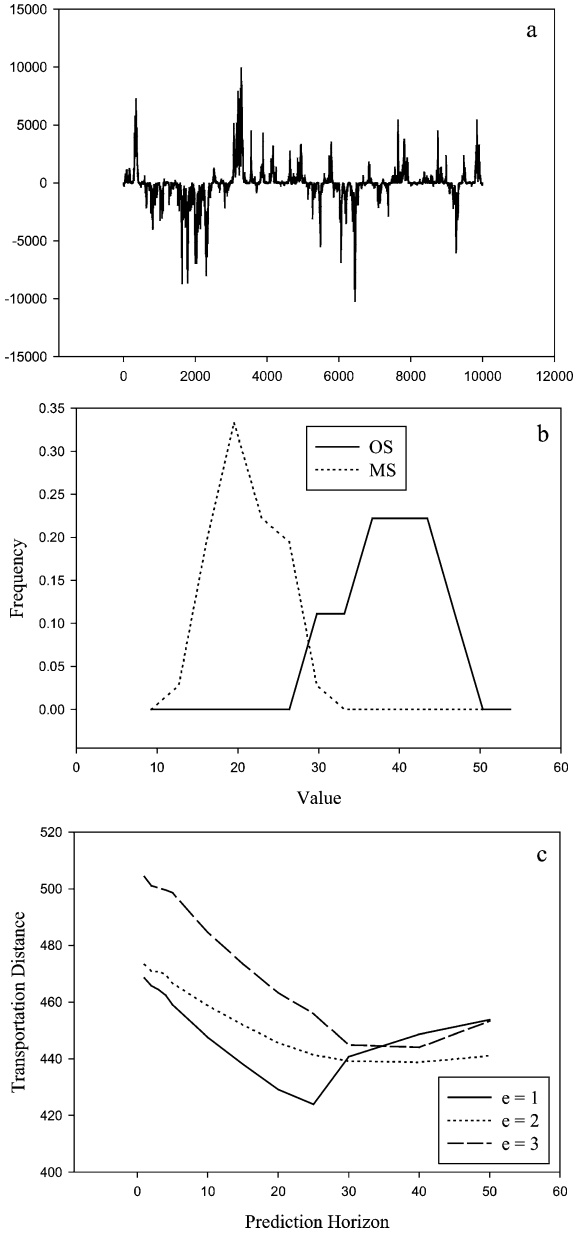

Fig. 3. Nonlinearly distorted autoregressive process: (a) time series, (b) transportation distance function distributions ($e = 3$) and (c) k-step prediction profile.

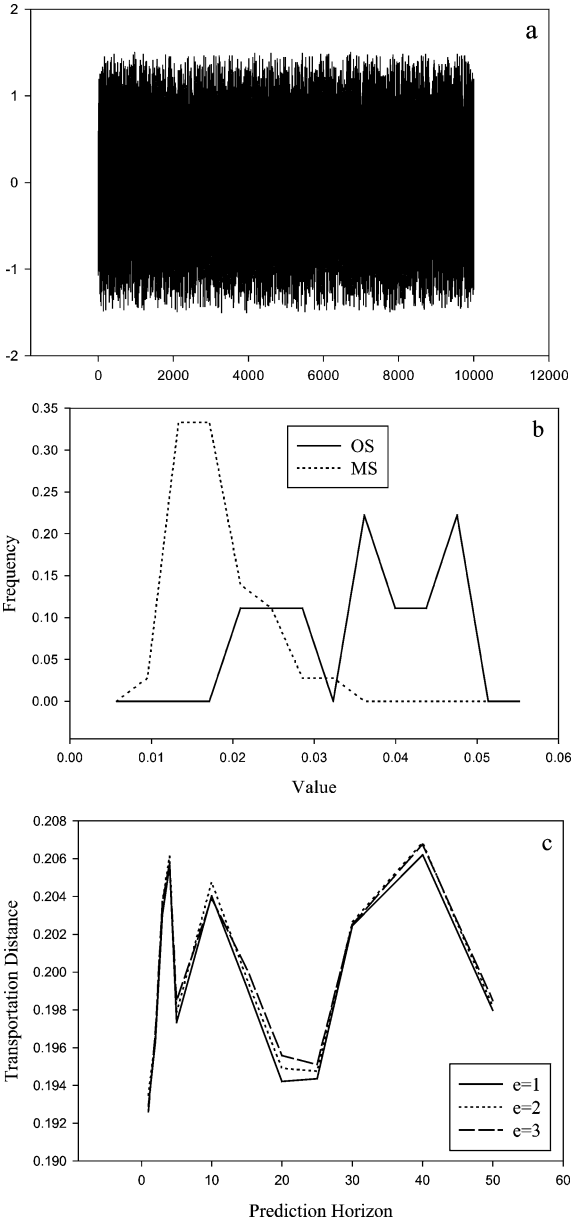

Fig. 4. Noisy sine limit cycle: (a) time series, (b) transportation distance function distributions ($e = 2$) and (c) k-step prediction profile.

where x_1 denotes location and x_2 velocity [25]. The parameter and noise combination of $\mu = 1$ and $\varepsilon = N(0, 1)$, respectively, makes the series weakly nonlinear [25]. The weak nonlinearity is captured by the first step of our framework as expected (Fig. 5(b)). The second step of our method does not provide conclusive answer on the stochastic nature of the process, although the transportation distance versus prediction horizon profile is certainly non-monotonic over

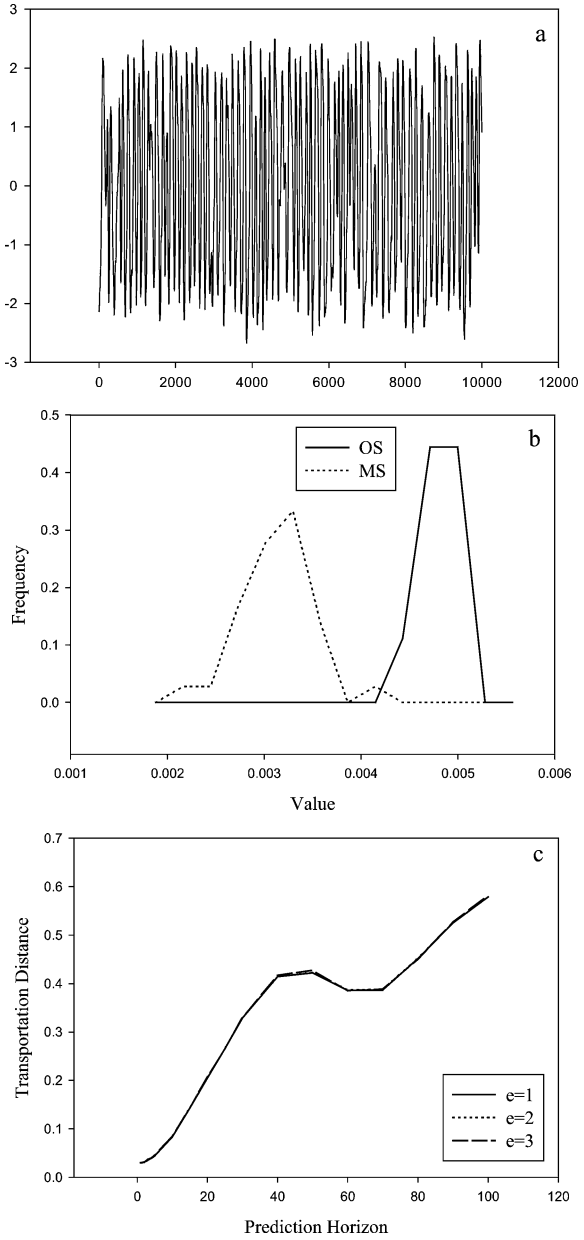

Fig. 5. Stochastic Van der Pol oscillator: (a) time series, (b) transportation distance function distributions ($e = 3$) and (c) k-step prediction profile.

the whole prediction horizon. It is argued that the monotonic behavior up to lag 40 (which could be misleading) is probably related to the dominant zone of oscillation of this system (interestingly, the first minimum of the mutual information also occurs at lag = 40).

5. Santa Fe Institute competition series

To further demonstrate the robustness and potential of the proposed two-step framework, we applied our method on the Data sets A and D1 of the Santa Fe Institute Competition series, which have been extensively analyzed in the literature with different algorithms [7].

Example 7. Data set A

This univariate time series (Fig. 6(a), top row) consists of observations from a far-infrared laser experiment, approximately described by three coupled nonlinear differential equations with Lorenz-like dynamics [10]. The OS and MS distributions remain separate (Fig. 6(b), top row) demonstrating the inherent nonlinearity in the series. Fig. 6(c) (top row) confirms the chaotic deterministic behavior of the underlying dynamics. The conclusions agree with the results of Casdagli and Weigend [5] and Paluš [15].

Example 8. Data set D1

This series (Fig. 6(a), bottom row) was numerically generated by driving a particle in a four-dimensional nonlinear multiple-well potential (nine degrees of freedom) with a small nonstationary drift in the well depths [7]. Due to a small Gaussian drift in one of the parameters, the system is referred in the literature as an "approximately deterministic" chaotic system [5]. The original series consists of 50 000 points. To limit our computational burden in this work we used only 10 000 points. Before proceeding to our results, we would like to mention some of the earlier researchers' experience on this data set. Casdagli and Weigend [5] mentions: "Distinguishing (dimensionality of) nine (deterministic chaos) from infinity (chaos) is beyond the reach of a DVS algorithm that employs simple local linear model." Similarly, Paluš [15] was able to detect only nonlinearity but could not reject any of the following hypotheses: nonlinear stochasticity, nonlinear determinism and chaoticity. Fig. 6(b) (bottom row) conspicuously depicts the presence of non-

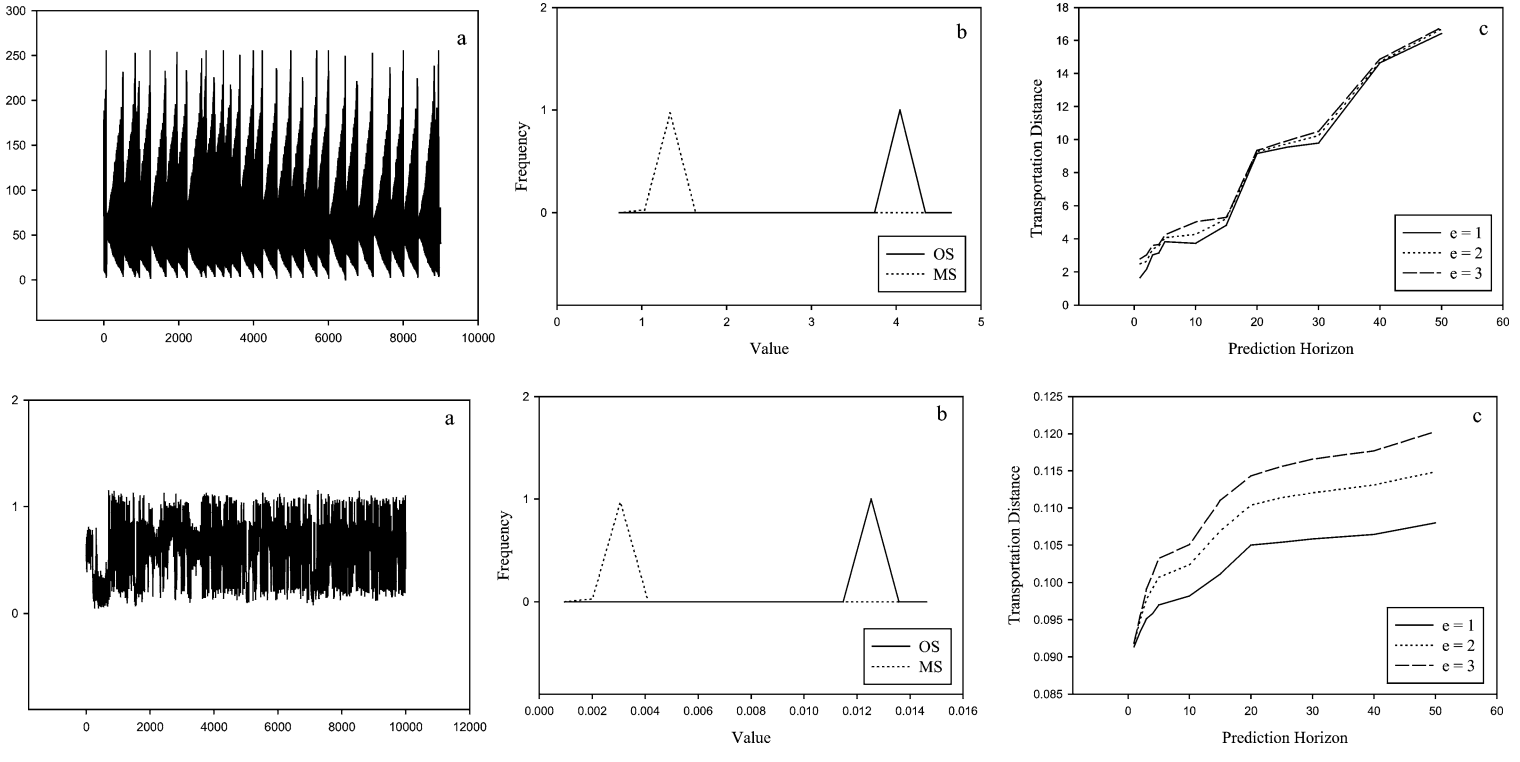

Fig. 6. Santa Fe competition data Series A (top row) and Series D1 (bottom row): (a) time series, (b) transportation distance function distributions ($e = 3$) and (c) k-step prediction profile.

linearity in the series. Fig. 6(c) (bottom row) showing the short-term prediction profile, clearly depicts the inherent chaotic nature of the data. This example demonstrates the power of our framework to differentiate between high-dimensional chaos and stochastic underlying dynamics. Since many natural processes are expected to exhibit high-dimensional determinism such an attribute of a detection methodology is very important for practical applications.

6. Conclusions

Motivated by the transportation distance function, in this Letter we proposed a robust framework to detect nonlinearity and chaoticity in a time series. Application of this framework to known examples suggests that it is able to detect nonlinearity and chaoticity not only in the presence of noise but also in the case of high-dimensional deterministic systems. It is also unlikely that this framework can be fooled by correlated noise or distorted linear stochastic processes (static nonlinearity). Theiler [24] comments that "It is, of course, impossible to provide an absolutely definitive resolution of whether or not a given finite data set is chaotic". Although this is true, we believe that proper application of the proposed framework can at least eliminate any possibility of spurious dimension or Lyapunov exponent computation.

Acknowledgements

This work was partially supported by NSF (grant ATM-013094) and NASA (grants NAG5-7715 and NAG8-1519) and the computational resources were provided by the Minnesota Supercomputing Institute. All these sponsors are gratefully acknowledged. The authors want to thank Richard Moeckel, Joydeep Bhattacharya, Thomas Schreiber, and Rainer Hegger for useful guidance and discussion during the course of this work.

References

[1] H.D.I. Abarbanel, Analysis of Observed Chaotic Data, Springer, New York, 1996.
[2] J. Bhattacharya, P.P. Kanjilal, Physica D 132 (1999) 100.
[3] J. Bhattacharya, P.P. Kanjilal, Eur. Phys. J. B 13 (2000) 399.
[4] M. Casdagli, J. R. Statist. Soc. Series B 54 (2) (1991) 303.
[5] M. Casdagli, A.S. Weigend, Exploring the continuum between deterministic and stochastic modeling, in: A.S. Weigend, N.A. Gershenfeld (Eds.), Time Series Prediction: Forecasting the Future and Understanding the Past, in: Santa Fe Institute Studies in the Sciences of Complexity, Proceedings, Vol. XV, Addison–Wesley, Reading, MA, 1993, p. 345.
[6] C. Diks, J.C. van Houwelingen, F. Takens, J. DeGoede, Phys. Lett. A 201 (1995) 221.
[7] N.A. Gershenfeld, A.S. Weigend, The future of time series: learning and understanding, in: A.S. Weigend, N.A. Gershenfeld (Eds.), Time Series Prediction: Forecasting the Future and Understanding the Past, in: Santa Fe Institute Studies in the Sciences of Complexity, Proceedings, Vol. XV, Addison–Wesley, Reading, MA, 1993, p. 1.
[8] P. Grassberger, I. Procaccia, Phys. Rev. Lett. 50 (1983) 346.
[9] R. Hegger, H. Kantz, T. Schreiber, Chaos 9 (1999) 413.
[10] U. Hübner, C. Weiss, N.B. Abraham, D. Tang, Lorenz-like chaos in NH_3-FIR lasers, in: A.S. Weigend, N.A. Gershenfeld (Eds.), Time Series Prediction: Forecasting the Future and Understanding the Past, in: Santa Fe Institute Studies in the Sciences of Complexity, Proceedings, Vol. XV, Addison–Wesley, Reading, MA, 1993, p. 73.
[11] H. Kantz, T. Schreiber, Nonlinear Time Series Analysis, Cambridge Univ. Press, Cambridge, 1997.
[12] M.B. Kennel, S. Isabelle, Phys. Rev. A 46 (6) (1992) 3111.
[13] Matlab 5.3, Mathworks, 1999.
[14] R. Moeckel, B. Murray, Physica D 102 (1997) 187.
[15] M. Paluš, Identifying and quantifying chaos by using information-theoretic functionals, in: A.S. Weigend, N.A. Gershenfeld (Eds.), Time Series Prediction: Forecasting the Future and Understanding the Past, in: Santa Fe Institute Studies in the Sciences of Complexity, Proceedings, Vol. XV, Addison–Wesley, Reading, MA, 1993, p. 387.
[16] M. Paluš, Physica D 80 (1995) 186.
[17] M. Paluš, Physica D 93 (1996) 64.
[18] A. Provenzale, L.A. Smith, R. Vio, G. Murante, Physica D 58 (1992) 31.
[19] T. Schreiber, A. Schmitz, Phys. Rev. Lett. 77 (4) (1996) 635.
[20] T. Schreiber, A. Schmitz, Phys. Rev. E 55 (5) (1997) 5443.
[21] T. Schreiber, A. Schmitz, Physica D 142 (2000) 346.
[22] G. Sugihara, R.M. May, Nature 344 (1990) 734.
[23] J. Theiler, S. Eubank, A. Longtin, B. Galdrikian, J.D. Farmer, Physica D 58 (1992) 77.
[24] J. Theiler, Phys. Lett. A 196 (1995) 335.
[25] J. Timmer, S. Häussler, M. Lauk, C.-H. Lücking, Chaos 10 (2000) 278.
[26] A.A. Tsonis, Chaos from Theory to Applications, Plenum, New York, 1992.